Effect of Annealing on the Curie Temperature in the Bulk Amorphous Alloys

BARTLOMIEJ JEZ*

Institute of Physics, Faculty of Production Engineering and Materials Technology, Czestochowa University of Technology, 19 Armii Krajowej Str., 42-200 Czestochowa, Poland

The paper presents results of research for volumetric amorphous alloys $Fe_{61+x}Co_{10-X}Y_8W_1B_{20}$ where x = 0,12 in the shape of plater of 10mm x 5mm x 0.5mm diameter. Amorphous Samales were annealed at 953K for 10 minutes what caused their partial crystallization. As a result of the thermal interference in the volume of alloys, three different crystalline phases were formed aFe, Fe_5Y and Fe_3B. For samples after solidification and after thermal treatment thermomagnetic studiem were conducted. For amorphous alloys, only one ferro-paramagnetic transition was visible, and for the alloys after the isothermal annealing process there were two inflections on the curve $.\mu_0M_s$ (T) corresponding to the two Curie temperatures. These intersections came from two amorphous phases. As a result of the research, it was found that these alloys crystallized in the primal crystalization. Crystallization was the reason for the increase of the first Curie temperature of the amorphous matrix while retaining its decrease with cobalt additive. The value of the second Curie temperature in the alloys after heating was found to depend mainly on the size of the crystallization products and in particular on the Fe_5Y crystallite size.

Keywords: nanocrystalline materials, amorphous alloys, isothermal annealing, Curie temperature

Conventional polycrystalline alloys are one of the most widespread materials in the world. Structures of countless grades of steel or aluminum are virtually impossible to replace by any other materials. On a macroscopic scale, the cost of materials is extremely important. Production of quality materials in conventional form is very well controlled and relatively cheap, even in the case of metal composite materials [1-4]. By moving from macroscopic engineering applications to precise and specialized products, production costs become less and less important, and more and more roles take over the properties of the materials produced. In many industries, emphasis is placed on selected properties. Magnetic properties are extremely important for different applications. At this point, polycrystalline materials often do not have satisfactory properties In this field. The answer to the search for materials that meet the high demands on the magnetic properties of alloys are rapid cooled materials [1,5-10]. Despite the identical chemical composition, these materials have completely different properties than their crystalline counterparts. Research on this type of material has been going on for several decades. The beginnings of quick-cooled alloys were not impressive. Despite the good magnetic properties, the problem was the form of material obtained. The first alloys for which an amorphous structure was obtained were made in the form of tapes of thicknesses of around 50 μm. The liquid melt casting method on the rotating cylinder allows very high cooling rates (10^5 – 10^6 K/s) what gives a very good chance of obtaining an amorphous structure for many chemical compositions [11-25]. Unfortunately, this small dimension drastically limited the ability to use on an industrial scale. In the following years new methods of production and new chemical compositions were created, which enabled the formation of amorphous structure. The research of many researchers and in particular A. Innue led to a breakthrough in the production of fast-cooled alloys. Determination of the principles during the production of amorphous alloys (atomic radius difference of main components, negative mixing heat and more than 3 alloy components), and the emergence of new manufacturing methods have resulted in the development of many new amorphous alloy groups [26-29]. Those materials are called bulk amorphous materials [30-33]. Currently, there are methods to produce alloys of a few centimeters in thickness. This has a tremendous impact on the wide application of industrial scales. Rapid cooling methods allow not only alloys with an amorphous structure but also alloys that are some kind of link between crystalline and amorphous structures - these are nanocrystalline alloys [34-36]. Such materials are characterized by very good magnetic properties such as low coercivity or high saturation magnetization [37-39].

Alloys of this kind can be achieved in several ways. There are known methods such as chemical methods of vapor deposition, sonochemistry), spraying methods, mechanical synthesis or hydration methods [40-46]. Often nanocrystalline materials are obtained using rapid cooling. This can be done in one or two steps. The one-step process of producing nanocrystalline materials is difficult to achieve. The problem is to choose a suitable cooling rate that will slow down the crystallization process but not in 100%. In this case, crystalline phases can be formed in the amorphous matrix. Unfortunately, the cooling rate should be determined empirically for each chemical composition, which presents many difficulties. However, this is possible to achieve and this lowers the cost of producing such materials. Currently, materials of this type are produced in two stages. The first step is the rapid cooling of the melt to obtain an amorphous structure. The second step is to temper the amorphous alloy at the right temperature and at the right time. These parameters affect the rate of seed growth (from the crystalline nuclei formed during the formation of the amorphous structure) and the increase in the number of grains (nucleation speed of the crystalline phase of the amorphous matrix). The nanocrystalline alloy will have different properties depending on the size of the obtained grains and the amount of grain. It is therefore important to conduct a study to determine the appropriate temperature and time of annealing.

* email: bartek199.91@o2.pl

An important factor in the production of nanocrystalline alloys is the chemical composition of the alloy. The elements present in the material determine the properties of the alloy obtained and determine the Glass forming ability. It is apparent that some elements are exceptionally resistant to amorphous conditions, such as nickel, which reaches an amorphous state at a cooling rate above 10^9 K /s. It is therefore important to select a chemical composition that allows for the formation of an amorphous structure, possibly partially crystallized. In this paper, an attempt has been made to produce a nanocrystalline alloy using a two-step process, thus by heating the amorphous alloy. An alloy with a chemical composition $Fe_{61+x}Co_{10-x}Y_8W_1B_{20}$ dla x= 0,1,2 was used.

Experimental part

Amorphous Allom of composition $Fe_{61+x}Co_{10-x}Y_8W_1B_{20}$ (where x= 0,1,2) were prepared Rusing injection casting. The first stage of production is weighing ingot components. The ingot used for further processing has been melted down in an arc furnace. The temperature of several thousand °C ensures the melting of all chemical components. The appropriate melting technique and several repetitions of the process ensure good mixing of the ingot components, which guarantees a uniform distribution of the elements and the reproducibility of the amorphous alloys obtained. It is also important to accurately weight the components, especially for low-alloying elements of the order of several percent, which can drastically change the finite properties of the nanocrystalline alloy. Melting is carried out in a protective atmosphere of argon. Before the melting of the ingot, pure titanium is smelted to absorb the residual oxygen from the vacuum chamber present in the furnace. The injection method allows you to obtain a melt cooling rate of the order of 10^2 K/s. This speed does not allow for the vitrification of any chemical composition but is sufficient for many chemical formulas. The method allows for the production of amorphous alloys with a thickness of over 1 mm which gives the possibility of wider use as for amorphous tapes. Forms used in the method allow the production of samples in the form of bars and plates. For the purposes of this study, plates with a thickness of approximately 0.5 mm were manufactured. Lower plate thickness is a greater guarantee of amorphous state. The alloy was produced in a vacuum chamber. After producing a high vacuum, argon is flushed into the chamber. The protective atmosphere created by this gas increases the guarantee of obtaining the desired alloy of the appropriate purity without the unwanted oxides on the surface of the sample. The insert placed in the quartz capillaries was melted by vortex currents. Figure 1 shows a diagram showing the course of molten alloy injection into a copper mold.

The obtained platelet specimens were subjected to a study to determine the type of structure obtained. X-ray diffraction was used. Tests were carried out using an automated X-ray machine (Brucker, D8 Advance). The apparatus is equipped with a solid state counter and an X-ray lamp CuKα. Studies were conducted for 2Θ angle ranking from 30 to 100° with 7 s for measurement step (resolution 7s/0.02°).

Subsequently, the resulting plates were finely divided into a powdered form. Powder was also subjected to X-ray diffraction studies. After assuring that the amorphous structure was obtained, powder samples were tested using Faraday's magnetic balance. After these measurements, the obtained samples in powder form and plates were subjected to an isothermal annealing process. Samples

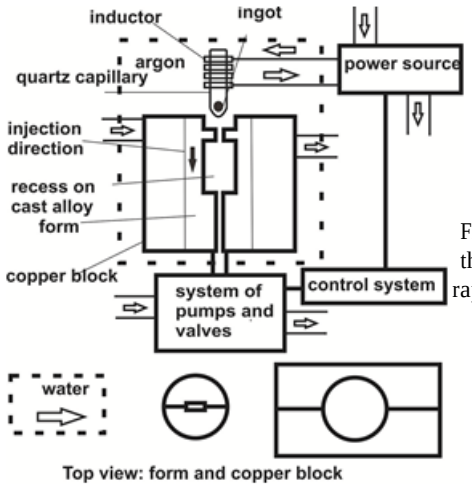

Fig.1. Scheme for the production of rapid-cooled alloys by injection casting

were heated at a temperature close to crystallization of 953 K for 10 min. Samples in the form of powder were subjected to structural studies (X-ray diffraction). The crystallite size was estimated using the Sherrer formula (1):

$$D = (\lambda * K)/2(_1 o\ cos\Theta \qquad (1)$$

K- shape coefficient Scherrera (K = 0.91);

λ- characteristic wave lenght;

B_0 - Half-width at half-peak intensity (background analysis included);

Θ- Bragg angle.

Results and discussions

Figures 2 and 3 show X-ray diffraction patterns obtained for samples in the post-solid state.

All of the diffraction patterns in figure 2 can be distinguished by the reflections associated with the existence in volume volumes of ordering between long-range atoms. These reflections are quite low intensity, suggesting that they are very small in proportion to the whole sample. Based on the analysis of these diffractograms, it was found that these are the oxides formed by the melt clotting process and therefore the samples were subjected to a mechanical cleaning process using fine grained sandpaper with a gradation of 1000 and then subjected to washing in an ultrasonic cleaner. After this process, the surface of the sample was crushed in an agate mortar. The powder thus obtained was re-examined using an X-ray machine (fig. 3).

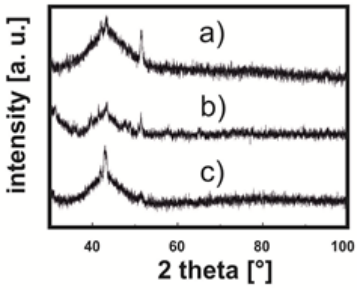

Fig. 2. XRD images for a 0.5 mm thick plate surface in as-solidified state:
a)$Fe_{61}Co_{10}Y_8W_1B_{20}$,
b) $Fe_{62}Co_9Y_8W_1B_{20}$,
c) $Fe_{63}Co_8Y_8W_1B_{20}$

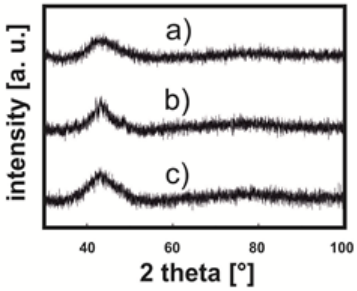

Fig. 3. X-ray diffraction patterns measured for a powdered alloy made from a 0.5 mm thick plate of the composition:
a) $Fe_{61}Co_{10}Y_8W_1B_{20}$,
b) $Fe_{62}Co_9Y_8W_1B_{20}$,
c) $Fe_{63}Co_8Y_8W_1B_{20}$,

The x-ray diffraction patterns shown in figure 3 are very similar. Only a wide blurry maximum is typical for materials of an amorphous structure [47]. This maximum is commonly referred to as the amorphous halo resulting from the dispersion of X-rays on chaotically spaced atoms in the volume of the melt. Powders used in X-ray studies (fig. 3) were subjected to a 953K thermal treatment over 10 min. The designed isothermal soaking process was supposed to produce crystalline grains of not more than 100 nm in volume. As indicated by the analysis of the diffraction patterns shown in figure 4, the obtained after thermal treatment samples were polycrystalline materials.

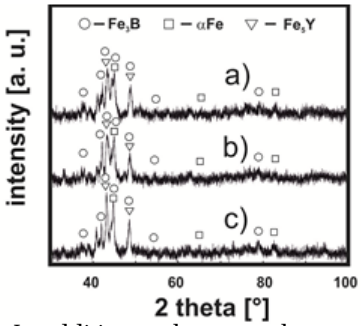

Fig. 4. X-ray diffraction patterns measured for a powdered alloy made from 0.5 mm thick plate after heating at 953 K for 10 min for composition:
a) $Fe_{61}Co_{10}Y_8W_1B_{20}$,
b) $Fe_{62}Co_9Y_8W_1B_{20}$,
c) $Fe_{63}Co_8Y_8W_1B_{20}$

In addition to the amorphous matrix, several crystalline phases could be distinguished in the volumes of these alloys: aFe, Fe_3B and Fe_5Y. Phase aFe is stable chase and Fe_3B and Fe_5Y are considered as metastable [48]. As for the phase fraction aFe on the magnetic properties of alloys is the presence of particles of size up to 50 nm affect the decrease of the coercive field and to increase the saturation magnetization. However, the designated metastable phases are not magnetically soft phases. It should be noted that the Fe_5Y phase is considered to be a semi-hard magnetic phase, which, with an increased share in the volume of the alloy, significantly deteriorates its main magnetically soft properties. For studiem alloys $Fe_{61+x}Co_{10-x}Y_8W_1B_{20}$ (x = 0, 1, 2) tere were no obvious influence of x on the emergencje of crystalline phases. The designed isothermal annealing process (953K / 10min) gave the possibility of producing samples with very similar structure and similar dimensions of crystallization products. Using the Scherrer method, the crystallite size for each phase was determined (table 1).

As indicated in table 1, the critical size of produced in crystallite alloy volume does not exceed 60 nm. For alloys where x = 0 and 2 the average particle size of the phases aFe and Fe_3B estimated based on Scherrer's dependency is the same. In the case of Fe_5Y for the same samples average grain size differs for several nm (for x = 0 - 58nm, for x = 2 - 43nm). The smallest average grain size for all identified crystalline phases was estimated for the alloy $Fe_{62}Co_{10}Y_8W_1B_{20}$.

Temperature stability of magnetic properties was investigated using Faraday's magnetic balance. The curves of magnetic saturation polarization as a function of temperature for the test alloys in the form of powder in solidified state and after thermal treatment are shown in the figure 5.

Table 1

DATA OBTAINED FROM ANALYSIS OF X-RAY DIFFRACTION PATTERNS (FIGURE 4) USING THE SCHRISTER PATTERN FOR THE SAMPLES AFTER HEATING (953K/10 MIN)

Phase	αFe [nm]	Fe_5Y [nm]	Fe_3B [nm]
$Fe_{61}Co_{10}Y_8W_1B_{20}$	43	58	34
$Fe_{62}Co_9Y_8W_1B_{20}$	29	36	27
$Fe_{63}Co_8Y_8W_1B_{20}$	43	43	34

As shown in figure 5 (a state after solidification), the saturation magnetic polarization of course a function of temperature in both directions (higher and lower temperature) are very similar [49, 50]. Note that the curve towards higher temperatures practically coincides with the return curve, which demonstrates the good stability of the magnetic structure. In the test range from 300K to 850K, only one magnetic transition from ferro to paramagnetism is visible. This pattern of magnetic saturation saturation is mainly related to the amorphous structure, which determines the domain structure that is difficult to describe in this case. Therefore, the observed bending on the curve is mild and rather related to a certain range of Curie temperature. This means that in transitionless magnetic materials with soft magnetic properties, transition from ferromagnetic to paramagnetic can occur in a narrow temperature range. A completely different shape of the thermomagnetic curves as a function of temperature was observed for the samples of the melt tested after the isothermal soaking process. The designed heat treatment (953K / 10min) was supposed to produce 100 nm of fine crystalline grains in the volume of the melt. The selected temperature is close to the original crystallization temperature for a given group of alloys. It would therefore be expected that the crystallization would be one crystalline phase, and this is not the case (fig. 4). Figure 5d, e, f show thermomagnetic curves as a function of temperature for samples after isothermal baking (953K / 10min). It can be clearly seen that almost all of the amorphous matrix has been replaced by ferromagnetic

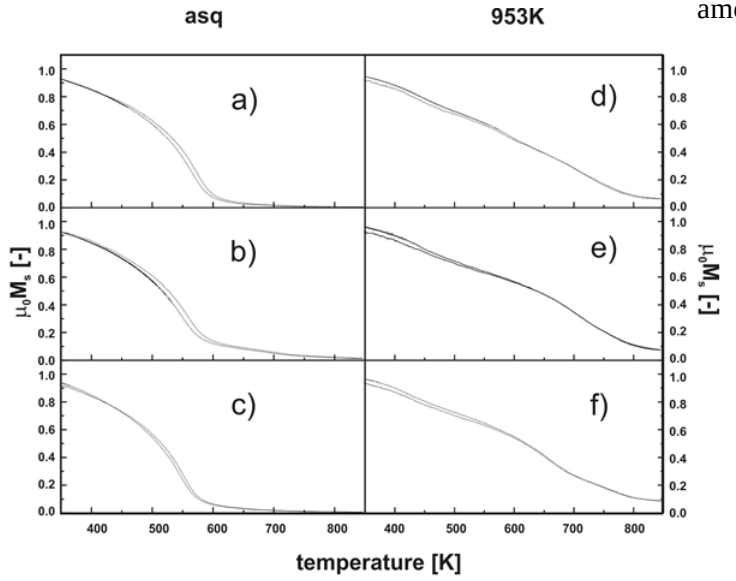

Fig. 5. Thermomagnetic curves for samples of tested alloys in solidified and heat-treated state (953°C/10 min.): as-solidified state - a), b), c), and after thermal treatment d) - f)

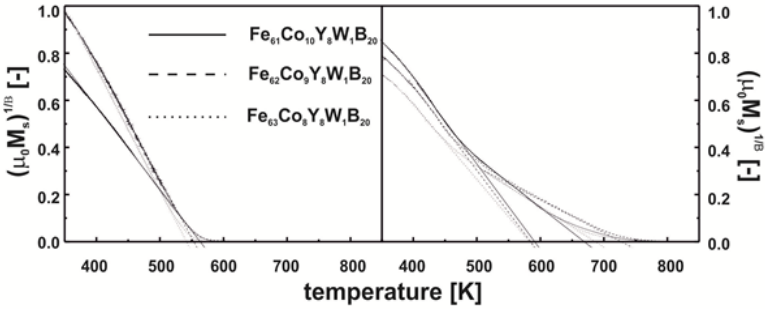

Fig. 6. Curie temperature for alloys in solidified state as well as first Curie temperature for alloys after isothermal baking is related to the order of close range between atoms

crystalline systems. It is obvious that from these results it is impossible to infer what crystal structure we are dealing with because in the given temperature range there are no sudden jumps of magnetic saturation polarization, typical of ferromagnetic crystalline systems. Based on the analysis of these curves, it is clear that the residual amorphous matrix of such chemical composition as that of solidified alloys remains unchanged in the volume of the alloy under test, which is why the tested alloys crystallize in the primary way. The primary crystallization mechanism itself assumes that a minimum of two products of differing compositions and non-starting alloys will be produced. In addition, from the shape of these curves, there are two Curie temperatures in the study area (fig. 6). For ferromagnetic materials meeting Heisberg's assumptions, a Curie temperature can be determined using a β factor of 0.36.

The data obtained from the analysis of thermomagnetic curves taking into account the critical factor b are summarized in figure 7.

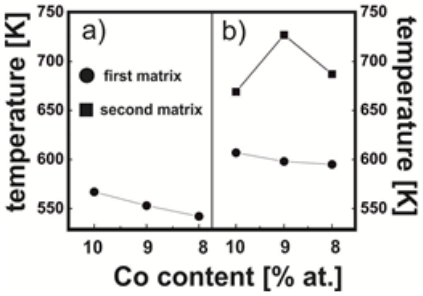

Fig. 7. Diagrams of curie temperature dependence on cobalt content in melt a) in solidified state b) after heat treatment (953K / 10min)

As for the alloy produced in the solidified state (having an amorphous structure), its curie temperature stability is good. In the case of the same alloys after the isothermal process, the first curie temperature stability corresponding to the first amorphous matrix is rather unstable. This is due to the small proportion of the volume of this amorphous matrix in the alloy. For samples in the solidified state and for the first amorphous matrix in the samples after heating, a Curie temperature change associated with the cobalt content of the alloy is observed. Cobalt has over 300K higher Curie temperature than iron, which affects the observed results. It should be noted, however, that the first Curie temperature for alloys after heating is nearly 60K higher than for solidified samples. The effect on this behavior of the first Curie temperature changes in the chemical order of the matrix and the content of the individual elements. It is known that in the alloys after annealing, three iron-rich crystalline phases were formed, and iron was then drawn from the amorphous matrix which resulted in a local increase in the cobalt content. Therefore, such a rise in Curie temperature is observed. The Curie temperature for the second amorphous matrix in the alloys after heating is completely different. Based on the analysis of the data in table 1, it can be concluded that the decisive parameter influencing Curie's temperature change is the crystallite size. It should be assumed that the average crystallite size can be a quantitative determinant of the contribution of a given crystalline phase in the volume of the investigated sample. Therefore, it can be assumed that the volume fraction of the phase αFe and Fe_3B In alloys $Fe_{61}Co_{10}Y_8W_1B_{20}$ and $Fe_{63}Co_{10}Y_8W_1B_{20}$ Is similar because average grain size is 43 nm and 34 nm, respectively. The change in the second Curie temperature for these two alloys is due to the increase in Fe_5Y phase grains. Of course, the above description of the influence of the average particle size on the curie's temperature property is related to the existence of the second amorphous matrix resulting from their existence. Curie's high temperature gradient for x = 1 is the result of significant crushing of the average crystallite dimension in the identified phases as compared to the previously described alloys where x = 0 and 2.

Conclusions

By using the liquid melt injection method, volumetric alloys can be produced of composition $Fe_{61+x}Co_{10-x}Y_8W_1B_{20}$ with amorphous structure and dimmensions 10mm x 5mm x 0.5mm.

Properly designed heat treatment process (953K / 10 min) gives the possibility of producing crystallization products of not more than 60 nm in $Fe_{61+x}Co_{10-x}Y_8W_1B_{20}$ alloys.

Three ferromagnetic crystalline phases were identified in the volume of the investigated alloys: soft magnetic aFe, and two metastable Fe_5Y (described as semi-hard magnetic) and Fe_3B (unordered).

In amorphous alloys there was one Curie temperature corresponding to the amorphous matrix whereas in the alloys after the heat treatment process, two curie temperatures from two amorphous.

Based on the analysis for nanocrystalline alloys, it was found that they crystallized in the primary way.

Changes in chemical compositions of amorphous matrixes after the annealing process are directly related to the crystallization products.

The sharp Curie temperature change for the second amorphous matrix in the $Fe_{62}Co_9Y_8W_1B_{20}$ alloy after heating is related to the smallest dimension of the crystallites.

References

1.LESZ, S., SZEWCZYK, R., SZEWIECZEK, D., BIENKOWSKI, A., J. Mater. Process. Tech. **157-158**, 2004, p. 743.
2.GAWDZINSKA, K., CHYBOWSKI, L., PRZETAKIEWICZ, W., Archives of Civil and Mechanical Engineering, **16**(3), 2016, p. 553.
3.GAWDZINSKA, K., Archives of Metallurgy and Materials, **58**(3), 2013, p. 659.
4.RICHTER, J., HUTCHINGS, I.M., WCLYNE, T., ALLSOPP, D.N., PENG, X., Materials Characterization, **45**(3), 2000, p. 233.
5.INOUE, A., SHEN, B.L., CHANG, C.T., Intermetallics, **14**, 2006, p. 936.
6.ASGAR, M,A., Mechanical Engineering Research Bulletin, **7,** 1984, p. 1.
7.SHEN, B., INOUE, A., Applied Physics Letters **85** (21), 2004, p. 4911.
8.KLEMENT, W., WILLENS, R.H., DUWEZ, P., Non-Crystalline Structure in Solidified Gold-Silicon Alloys, Nature, **187,** 1960, p.869.

9.MCHENRY, M.E., WILLARD, M.A., LAUGHLIN, D.E., Prog. Mater. Sci., **44**, 1999, p. 291.
10.LI, D.K., ZHANG, A.M., ZHU, Z.W., HU, Z.Q., Chinese Science Bulletin, **56** (36), 2011, p. 3926.
11.HASIAK, M., SOBCZYK, K., ZBROSZCZYK, J., CIURZYNSKA, W., OLSZEWSKI, J., NABIALEK, M., KALETA, J., ŒWIERCZEK, J., LUKIEWSKA, A., IEEE Trans. Magn. **11**, 2008, p. 3879.
12.WANG, W.H., DONG, C.H., Materials Science and Engineering R **44**, 2004, p. 45.
13.SOBCZYK, K., SWIERCZEK, J., GONDRO, J., ZBROSZCZYK, J., CIURZYNSKA, W., OLSZEWSKI, J., BRYGIEL, P., LUKIEWSKA, A., RZACKI, J., NABIALEK, M., J.Magn. Magn. Mater. **324**, 2012, p. 540.
14.INOUE, A., YANO, N., MASUMOTO, T., J. Mater. Science **19**, 1984, p. 3786.
15.LI, W., YANG, Y.Z., XU, J., Journal of Non-Crystalline Solids **461**, 2017, p. 93.
16.GRUSZKA, K., NABIALEK, M., SZOTA, M., BLOCH, K., GONDRO, J., PIETRUSIEWICZ, P., SANDU, A.V., MUSTAFA AL BAKRI, A.M., WALTERS, M., WALTERS, K., GARUS, S., DOSPIAL, M., MIZERA, J., Arch. Metall. Mater., **61**, 2016, p. 641.
17.NABIALEK, M., Arch. Metall. Mater., **61**, 2016, p. 439.
18.SUN, H.J., MAN, Q., DONG, Y.Q., SHEN, B., KIMURA, H., MAKINO, A., INOUE, A., J. Alloys Comp. **504**, 2010, p. 31.
19.CHIRIAC, H., LUPU, N., Physica B: Condensed Matter, **299**(3–4), 2001, p. 293.
20.NABIALEK, M., PIETRUSIEWICZ, P., BLOCH, K., SZOTA, M., Int. J. Mater. Res., **106**, 2015, p. 682.
21.DUWEZ, P., WILLENS, R.H., Transactions of the Metallurgical Society of Aime, **227**, 1963 p. 362.
22.CHEN, H.S., MILLER, C.E., Materials Reserch Bulletin, **11**, 1976, p. 49.
23.GONDRO, J., SWIERCZEK, J., BLOCH, K., ZBROSZCZYK, J., CIURZYNSKA, W., OLSZEWSKI, J., Physica B: Condensed Matter, **445**, 2014, p. 37.
24.SZOTA, M., Arch. Metall. Mater. **60** (4), 2015, p. 3095.
25.JEZ, B., NABIALEK, M., PIETRUSIEWICZ, P., GRUSZKA, K., BŁOCH, K., GONDRO, J., RZACKI, J., ABDULLAH, M. M. A. B., SANDU, A.V., SZOTA, M., JEZ, K., SALAGACKI, A., IOP Conf. Series: Materials Science and Engineering **209**, 2017, p. 012023.
26.BLOCH, K., NABIALEK, M., Acta. Phys. Pol. A **127**, 2015, p. 442.
27.GONDRO, J., ZBROSZCZYK, J., CIURZYNSKA, W., OLSZEWSKI, J., NABIALEK, M., SOBCZYK, K., SWIERCZEK, J., LUKIEWSKA, A., Archives of Metallurgy and Materials, **55**, no. 1 (2010), 85.
28.INOUE, A., KATO, A., ZHANG, T., KIM, S.G., MASUMOTO, T., Materials Transaction JIM, **32**, 1991, p. 609.
29.INOUE, A., ZHANG, T., MASUMOTO, T., Materials Transactions JIM, **31**, 1990, p. 177.
30.BLOCH, K., J. Magn. Magn. Mater.**390**, 2015, p. 118.
31.NABIALEK, M., PIETRUSIEWICZ, P., BLOCH, K., J. All. Comp. **628**, 2015, p. 424.
32.BLOCH, K., NABIALEK, M., Acta. Phys. Pol. A **127**, 2015, p. 413.
33.OLSZEWSKI, J., ZBROSZCZYK, J., HASIAK, M., KALETA, J., NABIALEK, M., BRYGIEL, P., SOBCZYK, K., CIURZYNSKA, W., ŒWIERCZEK, J., LUKIEWSKA, A., Journal of Rare Earths, **27**, no 4 (2009), 680.
34.NABIALEK, M., J. Alloys Comp. **642**, 2015, p. 98.
35.GRUSZKA, K.M., NABIALEK, M., BŁOCH, K., OLSZEWSKI, J., Nukleonika **60**, 2015, p. 23.
36.GONDRO, J., J. Magn. Magn. Mater. **432**, 2017, p. 501.
37.HAN, Y., CHANG, C.T., ZHU, S.L., INOUE, A., LOUZGUINE-LUZGIN, D.V., SHALAAN, E., AL-MARZOUKI, F., Intermetallics, **54**, 2014, p. 169.
38.HERZE, G., Scripta Metallurgica et Materialia, **33**, 1995, p. 1741.
39.HERZE, G., Acta Materialia, **61**, 2013, p. 718.
40.MAZALEYRAT, F., VARGA, L.K., J.Magn Mater., **215-216**, 2000, p. 253.
41.YANAI, T., YAMASAKI, M., NAKANO, M., FUKUNAGA, H., YOSHIZAWA, Y., Soft Magnetic Materials, **10**, 2003, p. 737.
42.GRACE, J.M., MARIJNISSEN, J.C.M.J., Aerosol Science, **25**, 1994, p.1005.
43.BENJAMIN, J.S., Metall. Trans., **1,**1970, p. 2943.
44.FROES, F.H., SURYANARAYANA, C., RUSSELL, K., LI, C.G., Mat. Sci. Eng. **A192/193**, 1995, p. 612.
45.MCGUINESS, P., SHORT, C., WILSON, A.F., HARRIS, I.R., J. Alloys Comp., **184**, 1992, p. 243.
46.ESTEVEZ, E., FILDER, J., SHORT, C., HARRIS, I.R., J. Phys., D **29**, 1996, p. 951.
47.GARUS, S., NABIALEK, M., BŁOCH, K., GARUS, J., Acta. Phys. Pol. A **126**, 2014, p. 957.
48.SOBCZYK, K., NABIALEK, M., OLSZEWSKI, J., BRYGIEL, P., CIURZYNSKA, W., ŁUKIEWSKA, A., LUBAS, M., SZOTA, M., Archives of Metallurgy and Materials, **53**, no. 3, 2008, p. 855.
49.GONDRO, J., ŒWIERCZEK, J., OLSZEWSKI, J., ZBROSZCZYK, J., SOBCZYK, K., CIURZYNSKA, W.H., RZYCKI, J., NABIALEK, M., Journal of Magnetism and Magnetic Materials, **324**, 2012, p. 1360.
50.BLOCH, K., NABIALEK, M., GRUSZKA, K., Rev. Chim.(Bucharest), **68**, no. 4, 2017, p. 698

Manuscript received: 18.01.2017